

Theoretical Investigations into Transition Metal–Group 13 Element Bonding: Comparison between Ruthenium Porphyrin and Ruthenium Carbonyl Diyl Compounds

Tobias Bollwein, Penelope J. Brothers,* Holger L. Hermann, and Peter Schwerdtfeger*

Department of Chemistry, The University of Auckland, Private Bag 92019, Auckland, New Zealand

Received July 8, 2002

Density functional calculations have been carried out to determine the structure and bonding for ruthenium porphyrin and carbonyl diyl complexes $(\text{CO})_4\text{Ru}-\text{EH}_{\text{eq}}$ (**1a–e**), $(\text{CO})_4\text{Ru}-\text{EH}_{\text{ax}}$ (**2a–e**), $(\text{Por})\text{Ru}-\text{EH}$ (**3a–e**), and for $(\text{Por})\text{Ru}-\text{E}(\text{trip})$ (**4a–e**, $\text{trip} = 2,4,6$ -triisopropylphenyl) with E being a group 13 element (E = B–Ti). Subsequent natural bond orbital (NBO) analyses have been applied to examine in detail the Ru–E bonding situation and the influence of the porphyrin ligand. The calculations reveal high Ru–E (E = B–Ti) bond dissociation energies, especially for the ruthenium boron bonds in **3a** and **4a**. The NBO analyses show E–Ru π -back-bonding is most significant in the case of boron. The influence of the porphyrin ligand on this π -back-bonding interaction is similar to the one demonstrated for carbonyl ligands; however, the σ -donation from E to Ru is stronger in the case of the porphyrin ligand.

Introduction

There has been a recent increase in interest in compounds containing transition metal–group 13 element bonds (M–E) for reasons relevant to both applied and fundamental research.^{1,2} A number of complexes bearing carbonyl and Cp* ligands have been synthesized over the past few years, mostly containing the transition metals Fe, Cr, W, Mn, Mo, and Pt bonded to group 13 elements.^{3–6} In contrast, only a few ruthenium–group 13 element bonded compounds have been isolated, for example the boryl compounds $[(\eta^5\text{-C}_5\text{H}_5)(\text{CO})_2\text{Ru}\{\text{BCl}$

$\{\text{NSiMe}_3\{\text{BCIN}(\text{SiMe}_3)_2\}\}]^6$ and $[(\eta^5\text{-C}_5\text{H}_5)(\text{CO})_2\text{Ru}-\text{B}(\text{NMe}_2)\text{B}(\text{Br})(\text{NMe}_2)]^7$ and the gallium diyl compound $\text{Ru}\{\text{GaCl}(\text{THF})_2\}\{\text{GaCl}_2(\text{THF})\}_2(\text{CO})_3$.⁸

The recent synthesis⁴ of $(\text{CO})_4\text{FeGaAr}^*$ sparked a controversy among synthetic and computational chemists that has developed into a more general discussion focused on the nature of the M–E bond in transition metal group 13 diyl compounds, $\text{L}_n\text{M}-\text{ER}$.^{5,9–12} One area of interest is the degree of ionic versus covalent character; the other concerns the π -back-bonding contribution in the M–E bond (Figure 1). The picture that emerges is that of a σ -interaction involving donation of the lone pair electrons on E to the d_z^2 orbital of the transition metal (Figure 1a), a weaker π -back-bonding contribution from the d_{xz} and d_{yz} orbitals of the latter into the p_x and p_y orbitals of E (Figure 1b), and a strong

(1) Reviews: (a) Linti, G.; Schnökel, H. *Coord. Chem. Rev.* **2000**, 206–207, 285. (b) Fischer, R. A.; Weiss, J. *Angew. Chem., Int. Ed.* **1999**, 38, 2830. (c) Wrackmeyer, B. *Angew. Chem., Int. Ed.* **1999**, 38, 771. (d) Braunschweig, H. *Angew. Chem., Int. Ed.* **1998**, 37, 1786. (e) Irvine, G. J.; Lesley, M. J. G.; Marder, T. B.; Norman, N. C.; Rice, C. R.; Robins, E. G.; Roper, W. R.; Whittell, G. R.; Wright, L. J. *Chem. Rev.* **1998**, 98, 2685.

(2) Review: Boehme, C.; Uddin, J.; Frenking, G. *Coord. Chem. Rev.* **2000**, 197, 249.

(3) (a) Jutzli, P.; Neumann, B.; Reumann, G.; Schebaum, L. O.; Stämmler, H.-G. *Organometallics* **1999**, 18, 2550. (b) Yu, Q.; Purath, A.; Donchev, A.; Schnökel, H. *J. Organomet. Chem.* **1999**, 584, 94. (c) Braunschweig, H.; Koster, M.; Wang, R. *Inorg. Chem.* **1999**, 38, 415. (d) Haubrich, S. T.; Powers, P. P. *J. Am. Chem. Soc.* **1998**, 120, 2202. (e) Jutzli, P.; Neumann, B.; Reumann, G.; Stämmler, H.-G. *Organometallics* **1998**, 17, 1305. (f) Cowley, A. H.; Lomeli, V.; Voigt, A. *J. Am. Chem. Soc.* **1998**, 120, 6401. (g) Braunschweig, H.; Kollan, C.; Englert, U. *Angew. Chem., Int. Ed.* **1998**, 37, 3179. (h) Braunschweig, H.; Kollann, C.; Englert, U. *Angew. Chem., Int. Ed.* **1998**, 37, 3179. (i) Schulte, M. M.; Herdtweck, E.; Raudaschl-Sieber, G.; Fischer, R. A. *Angew. Chem., Int. Ed. Engl.* **1996**, 35, 424.

(4) Su, J.; Li, X.; Crittendon, R. C.; Campana, C. F.; Robinson, G. H. *Organometallics* **1997**, 16, 4511.

(5) (a) Braunschweig, H.; Colling, M.; Kollann, C.; Merz, K.; Radacki, K. *Angew. Chem., Int. Ed.* **2001**, 40, 4198. (b) Fischer, R. A.; Schulte, M. M.; Weiss, J.; Zsolnai, L.; Jacobi, A.; Huttner, G.; Frenking, G.; Boehme, C.; Vyboishchikov, S. F. *J. Am. Chem. Soc.* **1998**, 120, 1237. (c) Weiss, J.; Stetzkamp, D.; Nuber, B.; Fischer, R. A.; Boehme, C.; Frenking, G. *Angew. Chem., Int. Ed. Engl.* **1997**, 36, 70.

(6) Braunschweig, H.; Kollann, C.; Klinkhammer, K. W. *Eur. J. Inorg. Chem.* **1999**, 1523.

(7) Braunschweig, H.; Koster, M.; Wang, R. *Inorg. Chem.* **1999**, 38, 415.

(8) Harakas, G. N.; Whittlesey, B. *Inorg. Chem.* **1997**, 36, 2704.

(9) (a) Braunschweig, H.; Colling, M.; Kollann, C.; Stämmler, H. G.; Neumann, B. *Angew. Chem., Int. Ed.* **2001**, 40, 2298. (b) Frenking, G. *J. Organomet. Chem.* **2001**, 635, 9. (c) Uddin, J.; Boehme, C.; Frenking, G. *Organometallics* **2000**, 19, 571. (d) Macdonald, L. B.; Cowley, A. H. *J. Am. Chem. Soc.* **1999**, 121, 12113. (e) Boehme, C.; Frenking, G. *Chem. Eur. J.* **1999**, 5, 2184. (f) Üffing, C.; Ecker, A.; Köppe, R.; Schnökel, H. *Organometallics* **1998**, 17, 2373. (g) Linti, G.; Köstler, W. *Chem. Eur. J.* **1998**, 4, 942. (h) Cotton, F. A.; Feng, X. *Organometallics* **1998**, 17, 128. (i) Ehlers, A. W.; Baerends, E. J.; Bickelhaupt, F. M.; Radius, R. *Chem. Eur. J.* **1998**, 4, 210. (j) Bickelhaupt, F. M.; Radius, U.; Ehlers, A. W.; Hoffmann, R.; Baerends, E. J. *New J. Chem.* **1998**, 1.

(10) Chen, Y.; Frenking, G. *J. Chem. Soc., Dalton Trans.* **2001**, 434.

(11) (a) Weiss, D.; Winter, M.; Merz, K.; Knüfer, A.; Fischer, R. A.; Fröhlich, N.; Frenking, G. *Polyhedron* **2002**, 21, 535. (b) Weiss, D.; Steinke, T.; Winter, M.; Fischer, R. A.; Fröhlich, N.; Uddin, J.; Frenking, G. *Organometallics* **2000**, 19, 4583. (c) Uhl, W.; Benter, M.; Melle, S.; Saak, W.; Frenking, G.; Uddin, J. *Organometallics* **1999**, 18, 3778. (d) Uhl, W.; Pohlmann, M.; Warchow, R. *Angew. Chem., Int. Ed.* **1998**, 37, 961.

(12) Udin, J.; Frenking, G. *J. Am. Chem. Soc.* **2001**, 123, 1683.

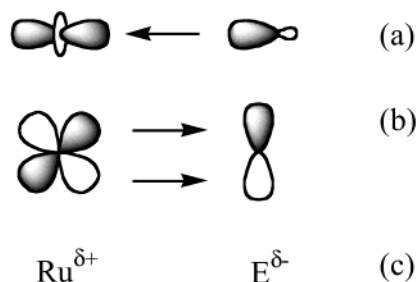


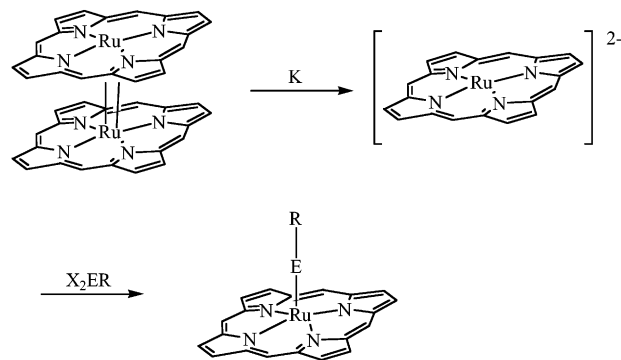
Figure 1. Schematic representation of the Ru–EH bonding situation: (a) σ -bonding, (b) π -bonding in two different planes, and (c) ionic interactions.

ionic interaction between these two elements dependent on the nature of E (Figure 1c).

The influence of the group R (H, Me, Cp, Cp*, Ph, SiR₃, F, NR₂) at the group 13 element has been investigated in theoretical and (to a more limited extent) experimental studies.^{9,10,12} However, the ligands present on the transition element are almost exclusively the strong π -acceptor carbon monoxide or, in some cases, the cyclopentadienyl ligand. Given that one of the areas of controversy surrounding the nature of the M–E bond is the extent of M–E π -bonding, the nearly ubiquitous presence of four or five very strong π -acceptor ligands in the transition metal coordination sphere will result in considerable competition for electron density at the metal and may well perturb any potential M–E π -bonding. There are only a very small number of group 13 diyl compounds that do not bear strong π -acceptors at the transition metal, either nickel homoleptic structures of the type Ni(ER)₄ or platinum complexes containing phosphine ligands.¹¹ The final point to make regarding the range of known or calculated transition metal group 13 diyl complexes is that the majority contain first-row transition metals (Cr, Mn, Fe, Ni). A small number of examples containing second- or third-row elements (Mo, W, Ru, Pt) have been reported experimentally,^{3–8} and theoretical studies have examined only examples containing Mo, W, Pd, or Pt.^{5,9,11} In a similar vein, most theoretical studies have focused on either boron or gallium as the group 13 element, with only a very small number of studies considering M–E bonding for the complete set of group 13 elements B, Al, Ga, In, and Tl.

In this work we examine by means of density functional theory (DFT) ruthenium–group 13 element bonded compounds in which the supporting ligand is a porphyrin dianion, giving complexes of the type (Por)Ru–ER. This study was undertaken for two reasons. First, in contrast to the CO ligand, the porphyrin ligand is not a strong π -acceptor and thus will not compete strongly with the ER ligand in (Por)Ru–ER complexes for π -electron density at the metal center. This study is the first to examine group 13 M–E bonding in metalloporphyrin complexes and is complementary to the raft of theoretical studies of complexes containing CO ligands discussed above. An obvious reason for the prevalence of group 13 transition metal carbonyl complexes is that the readily available carbonylmetal anions [(CO)_nM]^{x-} are useful synthons for M–E complexes through salt elimination reactions with group 13 halides. A second reason for studying the ruthenium porphyrin system is the availability experimentally of the Ru(0) porphyrin dianions^{13,14} [Ru(Por)]²⁻, which can potentially undergo

Scheme 1. Reduction of a Ruthenium Dimer and Following Metathesis Reaction with a Group 13 Dihalide



a metathesis reaction with alkyl group 13 dihalogenides X₂ER (E = B–Tl; X = Cl, Br) as shown in Scheme 1.^{14,15}

The second-row transition metal Ru(II) is intrinsically a good target for this study because of its higher propensity for π -back-bonding relative to first-row transition metals such as iron.¹⁶ Finally, again from an experimental standpoint, in contrast to pentacoordinated Fe(II) porphyrin species, which are usually paramagnetic,¹⁷ the corresponding Ru complexes are diamagnetic and more easily characterized by NMR. Thus in addition to their interest from a computational point of view, the ruthenium porphyrin complexes (Por)Ru–ER represent attractive and realistic synthetic targets for M–E complexes that do not bear strong π -acceptor ligands. The porphyrin complexes (Por)Ru–EH were investigated with R = H for computational simplicity, and the trip complexes (Por)Ru–E(trip)¹⁸ (trip = 2,4,6-triisopropylphenyl) were also studied since the bulky aryl ligand on the group 13 element E is again a realistic target for future synthesis. Both series of complexes (Por)Ru–ER (R = H, trip) were calculated for the complete set of group 13 elements B–Tl. Carbonyl ruthenium group 13 diyl complexes (CO)₄Ru–ER have not been investigated so far by either theory or experiment, in contrast to the isostructural iron complexes. We also studied the properties of the carbonyl complexes (CO)₄Ru–EH (E = B–Tl) containing the EH group in both the axial and equatorial positions. This allows a comparison between the first-row iron and second-row ruthenium (CO)₄M–EH systems and also a comparison of the different formal oxidation states of ruthenium, Ru(0) in the carbonyl compounds and Ru(II) in the porphyrin complexes. Due to the higher oxidation state of +II in the ruthenium porphyrin compounds, we expect a more ionic character of the Ru–E bond compared to the carbonyl species. As with the porphyrin species, both isomers of the carbonyl ruthenium com-

(13) Collman, J. P.; Brothers, P. J.; McElwee-White, L.; Rose, E.; Wright, L. J. *J. Am. Chem. Soc.* **1985**, *107*, 4570.

(14) Brothers, P. J. *Adv. Organomet. Chem.* **2000**, *46*, 223.

(15) Collman, J. P.; Brothers, P. J.; McElwee-White, L.; Rose, E. *J. Am. Chem. Soc.* **1985**, *107*, 6110.

(16) (a) Taube, H. *Angew. Chem.* **1984**, *96*, 315. (b) Taube, H. *Science* **1984**, *226*, 1028.

(17) (a) Scherlis, D. A.; Estrin, D. A. *Int. J. Quantum Chem.* **2001**, *87*, 158. (b) Collman, J. P.; Reed, C. A. *J. Am. Chem. Soc.* **1973**, *95*, 2048. (c) Spartalian, K.; Lang, G.; Collman, J. P.; Gagne, R. R.; Reed, C. A. *J. Chem. Phys.* **1975**, *63*, 5375. (d) Jamenson, G. B.; Molinaro, F.; Ibers, A.; Collman, J. P.; Brauman, J. I.; Rose, E.; Suslick, K. S. *J. Am. Chem. Soc.* **1980**, *102*, 3224.

(18) Tris-2,4,6-ⁱPr₃C₆H₂ ligand.

plexes were calculated for the full set of group 13 elements B–Tl.

Computational Methods

To analyze the bonding situation in the $(\text{CO})_4\text{Ru}-\text{EH}$, $(\text{Por})\text{Ru}-\text{EH}$, and $(\text{Por})\text{Ru}-\text{E}(\text{trip})$ species, we carried out DFT calculations using the Gaussian98 program package.¹⁹ As the porphyrin systems are rather large and we have chosen the more computer time intensive hybrid density functional of Becke, Lee, Yang, and Parr (B3LYP),²⁰ we adopted only a double- ζ sized valence basis set together with the corresponding pseudopotential parameter of Hay and Wadt (LANL2DZ)²¹ as implemented in Gaussian98. All structures were optimized at the B3LYP/LANL2DZ level of theory and were proven to be minima on the hypersurface by calculation of the second-order derivative matrix (Hessian). The geometry optimizations yielded the final structures of the following model compounds: $(\text{CO})_4\text{Ru}-\text{EH}_{\text{eq}}$ **1a–e**, $(\text{CO})_4\text{Ru}-\text{EH}_{\text{ax}}$ **2a–e**, $(\text{Por})\text{Ru}-\text{EH}$ **3a–e**, and $(\text{Por})\text{Ru}-\text{E}(\text{trip})$ **4a–e** (trip = 2,4,6-triisopropylphenyl). Dissociation energies were calculated as the difference between the molecule and the corresponding fragments (L_nRu and $\text{E}-\text{R}$) in their relaxed geometries. Atomic charges and orbital populations were calculated by applying the natural bond orbital (NBO) analysis scheme of Weinhold et al.²² The availability of the NBO data permits a comparison of the electronic situation on E of the ruthenium carbonyl with the porphyrin derivatives as well as with their iron analogues in the literature.⁹

For two compounds, $(\text{CO})_4\text{Ru}-\text{BH}_{\text{ax}}$ **2a** and $(\text{CO})_4\text{Ru}-\text{InH}_{\text{ax}}$ **2d**, we applied larger basis sets and different pseudopotentials to verify the LANL2DZ results. Namely, the Stuttgart ECP for Ru in conjunction with a large (31111/22111/411) pseudopotential basis set,²³ for In the Stuttgart ECP and a (31/31) pseudopotential basis set,²⁴ and for the other elements (H, B, C, O) an augmented correlation-consistent basis (aug-cc-pVDZ) of Dunning and co-workers²⁵ were used. Bonding parameters and Ru–E dissociation energies changed very little compared to the less computer time demanding LANL2DZ results.

Results and Discussion

Ruthenium Carbonyl Diyl Compounds $(\text{CO})_4\text{Ru}-\text{EH}$ (E = B–Tl; **1a–e**, **2a–e**). The optimized geom-

(19) Frisch, M. J.; Trucks, G. W.; Schlegel, H. B.; Scuseria, G. E.; Robb, M. A.; Cheeseman, J. R.; Zakrzewski, V. G.; Montgomery, Jr., J. A.; Stratmann, R. E.; Burant, J. C.; Dapprich, S.; Millam, J. M.; Daniels, A. D.; Kudin, K. N.; Strain, M. C.; Farkas, O.; Tomasi, J.; Barone, V.; Cossi, M.; Cammi, R.; Mennucci, B.; Pomelli, C.; Adamo, C.; Clifford, S.; Ochterski, J.; Petersson, G. A.; Ayala, P. Y.; Cui, Q.; Morokuma, K.; Malick, D. K.; Rabuck, A. D.; Raghavachari, K.; Foresman, J. B.; Cioslowski, J.; Ortiz, J. V.; Stefanov, B. B.; Liu, G.; Liashenko, A.; Piskorz, P.; Komaromi, I.; Gomperts, R.; Martin, R. L.; Fox, D. J.; Keith, T.; Al-Laham, M. A.; Peng, C. Y.; Nanayakkara, A.; Gonzalez, C.; Challacombe, M.; Gill, P. M. W.; Johnson, B.; Chen, W.; Wong, M. W. J.; Andres, L.; Gonzalez, C.; Head-Gordon, M.; Replogle, E. S.; Pople, J. A. *Gaussian 98*, Revision A.7; Gaussian Inc.: Pittsburgh, PA, 1998.

(20) (a) Becke, A. D. *J. Chem. Phys.* **1993**, *98*, 5648. (b) Lee, C.; Yang, W.; Parr, R. G. *Phys. Rev.* **1988**, *B37*, 785. (c) Bauschlicher, C. W.; Partridge, H. *Chem. Phys. Lett.* **1994**, *231*, 277. (d) Becke, A. D. *Phys. Rev. A* **1988**, *38*, 3098. (e) Vosko, S. H.; Wilk, L.; Nusair, M. *Can. J. Phys.* **1980**, *58*, 1200.

(21) (a) Dunning, T. H., Jr.; Hay, P. J. In *Modern Theoretical Chemistry*; Schaefer, H. F., III, Ed.; Plenum: New York, 1976; Vol. 3, p 1. (b) Hay, P. J.; Wadt, W. R. *J. Chem. Phys.* **1985**, *82*, 270. (c) Wadt, W. R.; Hay, P. J. *J. Chem. Phys.* **1985**, *82*, 284. (d) Hay, P. J.; Wadt, W. R. *J. Chem. Phys.* **1985**, *82*, 299.

(22) Glendening, E. D.; Reed, A. E.; Carpenter, J. E.; Weinhold, F. *NBO Version 3.1*; Gaussian Inc., Pittsburgh, PA, 1998.

(23) Andrae, D.; Haeussermann, U.; Dolg, M.; Stoll, H.; Preuss, H. *Theor. Chim. Acta* **1990**, *77*, 123.

(24) Bergner, A.; Dolg, M.; Kuechle, W.; Stoll, H.; Preuss, H. *Mol. Phys.* **1993**, *80*, 1431.

(25) (a) Dunning, T. H., Jr. *J. Chem. Phys.* **1989**, *90*, 1007. (b) Kendall, R. A.; Dunning, T. H., Jr.; Harrison, R. J. *J. Chem. Phys.* **1992**, *96*, 6769. (c) Woon, D. E.; Dunning, T. H., Jr. *J. Chem. Phys.* **1993**, *98*, 1358.

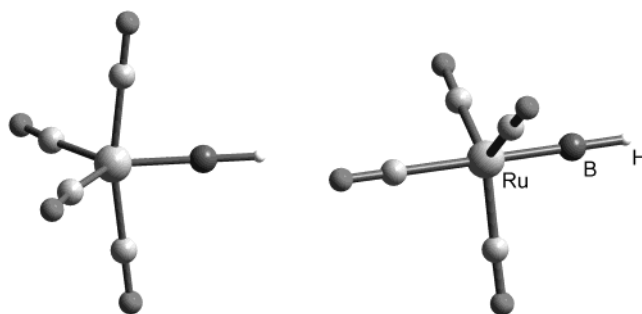


Figure 2. Optimized B3LYP geometries of the equatorial (**1a**, left) and axial (**2a**) isomers of $(\text{CO})_4\text{Ru}-\text{BH}$.

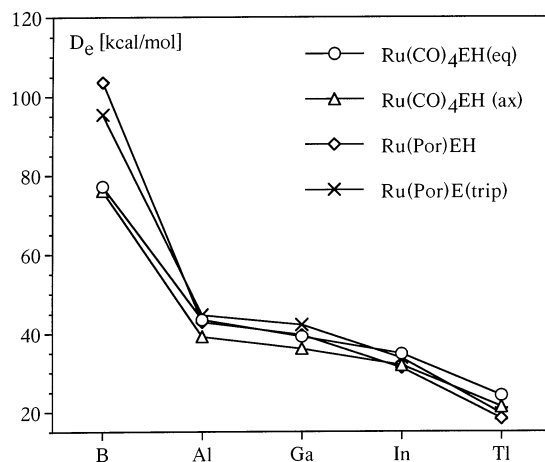


Figure 3. Ru–E bond dissociation energies (in kcal/mol) of the optimized diyl complexes **1a–4e**.

etries of the equatorial (**1a**) and axial (**2a**) borylene isomers of the ruthenium tetracarbonyl group 13 diyl compounds $(\text{CO})_4\text{Ru}-\text{BH}$ are shown in Figure 2, and the calculated structural parameters for **1a–e** and **2a–e** and bond dissociation energies (D_e) of the carbonyl complexes $(\text{CO})_4\text{Ru}-\text{EH}$ are listed in Table 1. Only the boron derivatives are presented in Figure 2 since the other structures are similar and vary mostly in the Ru–E bond length. The D_e values were calculated with respect to homolytic bond dissociation to the neutral fragment ER in the oxidation state I and the zerovalent ruthenium tetracarbonyl. $\text{Ru}(\text{CO})_4$ shows distorted T_d -like C_{2v} symmetry, and the ground state is of 1A_1 symmetry. This is in agreement with previous studies.²⁶

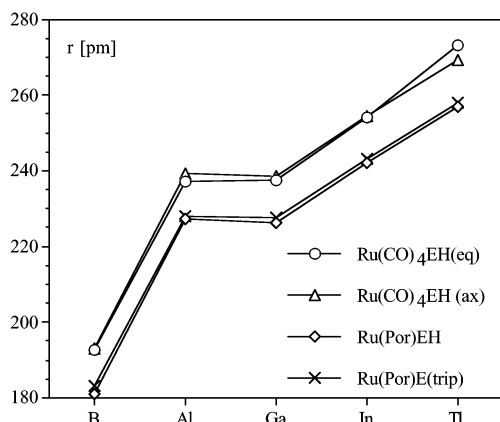
In contrast to most of the iron carbonyl compounds⁹ all the ruthenium carbonyl complexes with the group 13 element in an equatorial position are lower in energy (higher Ru–E dissociation energy) than their axial counterparts (Figure 3), and all are minima on their potential energy surfaces. The difference in energy observed between these isomers is 2.9–4.4 kcal/mol for E = Al–Tl and only 1.1 kcal/mol for the boron isomers. As expected, the dissociation energies of the ruthenium tetracarbonyl diyl compounds are lower than in the corresponding iron compounds,⁹ but the trend down the group regarding the group 13 elements remains the same as expected, i.e., B > Al > Ga > In > Tl. Interestingly, the Ru–B bond is predicted to be the most

(26) (a) Decker, S. A.; Klobukowski, M. *J. Am. Chem. Soc.* **1998**, *120*, 9342. (b) Li, J.; Schreckenbach, G.; Ziegler, T. *J. Am. Chem. Soc.* **1995**, *117*, 486. (c) Bogdan, P. L.; Weitz, E. *J. Am. Chem. Soc.* **1989**, *111*, 3163. (d) Bogdan, P. L.; Weitz, E. *J. Am. Chem. Soc.* **1990**, *112*, 639. (e) Ehlers, A. W.; Frenking, G. *Organometallics* **1995**, *14*, 423.

Table 1. Calculated Geometry Parameters and Bond Dissociation Energies of 1a–4e at the B3LYP/LANL2DZ Level of Theory

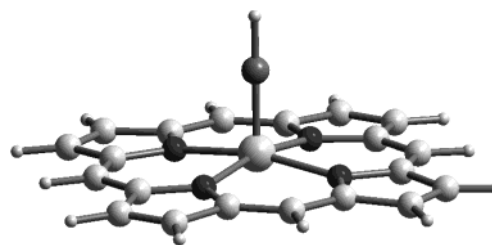
	$r(\text{Ru}-\text{E})^a$	$r(\text{Ru}-\text{CO}_{\text{eq}})$	$r(\text{Ru}-\text{CO}_{\text{ax}})$	$\alpha(\text{OC}_{\text{eq}}-\text{Ru}-\text{E})^b$	$\alpha(\text{OC}_{\text{ax}}-\text{Ru}-\text{E})$	$\alpha(\text{O}-\text{C}_{\text{eq}}-\text{Ru})$	$\alpha(\text{O}-\text{C}_{\text{ax}}-\text{Ru})$	$D_{\text{e}}(\text{Ru}-\text{E})^c$
(CO)₄RuEH_{eq}								
B (1a)	192.8	199.1	195.6	123.9	83.7	172.3	179.8	77.2
Al (1b)	237.2	195.4	194.8	120.0	85.6	179.8	178.9	43.5
Ga (1c)	237.5	195.3	194.9	120.0	86.2	179.4	179.2	39.2
In (1d)	254.0	194.7	194.8	119.7	86.3	178.0	178.9	34.8
Tl (1e)	273.0	193.9	195.2	116.5	88.4	175.7	179.5	24.2
(CO)₄RuEH_{ax}								
B (2a)	193.1 (190.3)	195.4 (195.2)	205.0 (206.2)	88.3 (88.3)	179.5 (179.6)	178.8 (178.8)	179.9 (179.9)	76.1 (77.0)
Al (2b)	239.3	194.5	195.3	87.6	179.6	177.8	180.0	39.2
Ga (2c)	238.5	194.7	195.0	87.8	179.7	177.9	180.0	36.1
In (2d)	254.3 (253.9)	194.6 (194.2)	193.7 (193.1)	87.7 (87.9)	179.7 (179.8)	177.3 (177.4)	180.0 (180.0)	31.9 (36.7)
Tl (2e)	269.3	195.0	191.3	88.0	179.8	177.1	180.0	21.3
	$r(\text{Ru}-\text{E})$	$d(\text{Ru}-\text{N})$	$\text{Ru}-\text{N}_4^g$	$D_{\text{e}}(\text{Ru}-\text{E})$				
(Por)^eRuEH								
B (3a)	181.2	207.7	21.8	103.5				
Al (3b)	227.1	207.1	17.6	42.8				
Ga (3c)	226.2	207.1	17.6	39.6				
In (3d)	242.1	207.0	15.7	31.2				
Tl (3e)	256.8	206.9	13.6	18.3				
(Por)RuEtrip^f								
B (4a)	183.0	207.7	21.8	95.3				
Al (4b)	228.0	206.9	15.7	44.7				
Ga (4c)	227.7	207.0	16.4	42.1				
In (4d)	243.3	206.8	13.6	33.7				
Tl (4e)	258.1	206.8	12.0	19.4				

^a Bond distance [pm]. ^b Angle [deg]. ^c Bond dissociation energy [kcal mol⁻¹]. ^d Values in parentheses are calculated with a larger basis set and different ECPs as described in Computational Methods. ^e Porphyrin. ^f See ref 18. ^g Displacement of the Ru from the porphyrin N₄ plane [pm].

**Figure 4.** Ru–E bond distances (in pm) of the optimized diyl complexes 1a–4e.

stable by a large margin, with much higher dissociation energies (**1a**, 77.2 kcal/mol; **2a**, 76.1 kcal/mol) than the complexes containing the heavier homologues (discussion below). A direct comparison of (CO)₄Ru–BH to a previous calculation at the B3LYP level for the iron tetracarbonyl borylene,¹⁰ (CO)₄Fe–BH, shows the Ru–B bond dissociation energy to be 12–18 kcal/mol lower depending on the basis set applied.

The Ru–E bond distances are usually larger than those observed for the iron analogues but again follow the same trend (B < Al ≈ Ga < In < Tl), as expected on the basis of the atomic radii of the group 13 elements (Figure 4). The CO ligands in the equatorial position of the axial isomers (**2a–e**) are bent toward the group 13 element ($\alpha(\text{C}_{\text{eq}}-\text{Ru}-\text{E})$ averages 88°), whereas the CO ligands in the axial positions of the equatorial isomers (**1a–e**) are only slightly bent toward E. The distances

**Figure 5.** Optimized B3LYP geometry of (Por)Ru–BH (**3a**).

of the CO fragments to the metal center vary between 191 and 195 pm except for the boron compounds **1a** and **2a**. In particular, the axial Ru(CO)₄BH (**2a**) exhibits a relatively long Ru–CO_{ax} bond of 205.0 pm due to the *trans* influence of the BH group. This result (B3LYP/LANL2DZ) is confirmed by an additional calculation with different pseudopotentials and larger basis sets (see Table 1).

Ruthenium Porphyrin Diyl Compounds (Por)–Ru–ER (E = B–Tl; R = H **3a–e; trip¹⁸ **4a–e**).** The calculated parameters and bond dissociation energies of the ruthenium porphyrin group 13 diyl compounds (Por)Ru–ER (**3a–e**, **4a–e**) are listed in Table 1. The optimized geometries of the two ruthenium porphyrin borylene compounds (Por)Ru–BR (R = H **3a**; trip **4a**) are shown as representative examples in Figures 5 and 6, respectively. The bond dissociation energies were calculated for the homolytic fragmentation to ER and the ruthenium(II) porphyrin. In contrast to the carbonyl species the ground state of (Por)Ru(II) has triplet symmetry (³E_g; D_{4h}) which is Jahn–Teller distorted toward D_{2h} symmetry and 28 kcal/mol more stable than the next singlet state. Again, this agrees well with

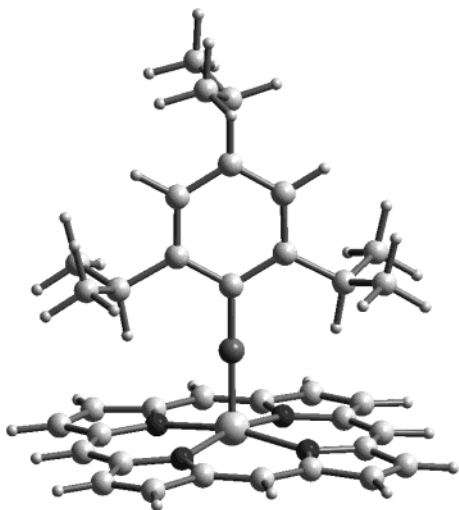


Figure 6. Optimized B3LYP geometry of (Por)Ru-Btrip (**4a**).

results published for the Ru(II) porphyrin fragment by Dixon and Matsuzawa also using DTF calculations.²⁷ Note that the ground state of (Por)Fe(II) was originally assigned to have 3E_g symmetry,^{27,28} but this was questioned by Kozlowsky et al.²⁹ and more recently by Liao and Scheiner,³⁰ who assigned the $^3A_{2g}$ state to be lower in energy. The energy difference between the two states is however only 0.12 eV,³⁰ in agreement with Mössbauer studies by Collman and co-workers.³¹ Similarly, in our case we find a $^3A_{1g}$ state to be only 0.6 kcal/mol above the Jahn–Teller distorted 3E_g state. For such small differences DFT calculations may not be reliable and more precise ab initio calculations are required to determine the correct ground state. This, however, is not significant to the following discussion.

Regarding the Ru–E bond dissociation energy of the compounds (Por)Ru–ER (E = B–Tl; R = H, trip; Figure 3), among the most striking features are the extremely high bond energies calculated for the boron derivatives **3a** (103.5 kcal/mol) and **4a** (95.3 kcal/mol). While the other values of the bond dissociation energy of (Por)Ru–EH (E = Al–Tl, **3b–e**) are comparable to those calculated for the corresponding ruthenium carbonyl molecules, the bond dissociation energy for (Por)Ru–BH_{eq} **3a** is predicted to be more than 26 kcal/mol higher than for (CO)₄Ru–BH **1a**. Compared to the next group 13 element containing compound (Por)Ru–AlR (**3b, 4b**), the dissociation energies for the boryls are twice as high. Furthermore, all the calculated Ru–E (E = B–Tl) bond distances (Table 1, Figure 4) of (Por)Ru–EH (**3a–e**) and (Por)Ru–E(trip) (**4a–e**) are more than 10 pm shorter than the corresponding carbonyl compounds (**1a–e**). As for the ruthenium carbonyl complexes, the trend down the group observed for the Ru–E bond length remains the same (B < Al ≈ Ga < In < Tl). The gallium compound (Por)Ru–GaH (**3c**) is calculated to contain a Ru–Ga(I) bond 17 pm shorter than that found in the

crystal structure of the diyl compound Ru{GaCl(THF)₂}{GaCl₂(THF)₂(CO)₃.⁸ As already mentioned, the difference of the bond strength of the ruthenium porphyrin borylene (**3a**) compared to the aluminum analogue (Por)Ru–AlH (**3b**) adds up to 60.7 kcal/mol, while the corresponding difference calculated for (CO)₄Ru–EH (E = B (**1a**), Al (**1b**)) is only 33.7 kcal/mol.

In general, similar results were calculated for the sterically more shielded trip compounds (Por)Ru–E(trip) (E = B–Tl, **4a–e**). For E = Al–Tl (**4b–e**) the bond dissociation energies are slightly higher (1.1–2.6 kcal/mol) than in (Por)Ru–EH (**3b–e**), while on the other hand the borylene (Por)Ru–B(trip) (**4a**) shows a lower Ru–E bond dissociation energy (by 8.2 kcal/mol) than (Por)Ru–BH (**3a**). This is most likely due to the increased influence of steric factors on the short Ru–B bond. Although the Ru–E bond distances of **4a–e** (E = B–Tl) are predicted to be 0.9–1.8 pm longer than in **3a–e**, these results show clearly that ruthenium porphyrin diyl compounds containing a trip ligand first should exhibit sufficient protection to shield the group 13 element and second can be expected to be thermodynamically stable, especially in the case of the borylenes.

All porphyrin compounds calculated here exhibit a linear geometry along the Ru–E–R bond axis. The out-of-plane displacement of the ruthenium atoms with respect to the four nitrogen atoms (Ru–N₄) is listed in Table 1. The largest values appear for the smallest group 13 atom E = B (21.8 pm, **3a, 4a**) with a steady decrease down the group to Tl. This trend corresponds with a decrease in the π -back-bonding contributions (see below) from B to Tl. There is no significant difference between the corresponding (Por)Ru–ER compounds **3a–e** (R = H) and **4a–e** (R = trip), but the out-of-plane displacement is on average 2 pm larger for R = H than for the trip-substituted molecules with E = Al–Tl. For both the borylene compounds the Ru–N₄ distances are 21.8 pm. The calculated ruthenium porphyrin complexes show D_{4h} symmetry for (Por)Ru–EH (**3a–e**) and slight distortions in the ring system toward C_s symmetry for (Por)Ru–E(trip) (**4a–e**) because of the trip ligand.

Bonding Analysis of Ruthenium Diyl Compounds. NBO analyses were carried out for the porphyrin compounds bearing EH substituents and for both the equatorial (**1a–e**) and the axial (**2a–e**) carbonyl isomers of (CO)₄Ru–EH. As there is a negligible influence of the hydrogen atom on the group 13 element p orbitals, the influence of the ligands toward the ruthenium–group 13 element bond can easily be determined. Previous studies showed that slightly stronger π -back-donations from the metal to E can be expected when using poor π -donor ligands at E, for example Me or Ph.^{2,10,12}

The calculated NBO parameters are given in Table 2. The atomic charges at the ruthenium atom range from $-0.4e$ (**2e**) to $-0.6e$ (**1b**) for the carbonyl compounds (**1a–e, 2a–e**), similar to the corresponding iron carbonyl complexes.^{2,12} This changes markedly for the higher oxidation state of ruthenium in (Por)Ru–EH (**3a–e**), where charges between $+0.3e$ (**3e**) and $-0.1e$ (**3c**) are now observed. Interestingly, in the complexes with boron (**3a**) and thallium (**3e**) ruthenium shows the most positive charge ($+0.3e$). A similar positive charge

(27) Matsuzawa, N.; Ata, M.; Dixon, D. A. *J. Phys. Chem.* **1995**, *99*, 7698.

(28) Delley, B. *Phys. B* **1991**, *172*, 185.

(29) Kozlowsky, P. M.; Spiro, T. G.; Bérces, A.; Zgierski, M. Z. *J. Phys. Chem. B* **1998**, *102*, 2603.

(30) Liao, M.-S.; Scheiner, S. *J. Chem. Phys.* **2002**, *117*, 205.

(31) Lang, G.; Spertalian, K.; Reed, C. A.; Collman, J. P. *J. Chem. Phys.* **1978**, *69*, 5424.

Table 2. Calculated NBO Parameters of 1a–4e at the B3LYP/LANL2DZ Level of Theory

	$q(\text{Ru})^a$	$q(\text{E})$	$q(\text{EH})$	$p_{x,y}(\text{E})^b$	$p_z(\text{E})^c$	$\Delta q(\sigma)^d$	$\Delta q(\pi)^e$	b/d^f
(CO) ₄ RuEH (eq)								
B (1a)	−0.46	0.39	0.25	0.59	0.80	0.84	−0.59	0.70
Al (1b)	−0.56	0.99	0.56	0.26	0.44	0.82	−0.26	0.32
Ga (1c)	−0.54	0.90	0.51	0.25	0.45	0.77	−0.25	0.33
In (1d)	−0.52	0.98	0.56	0.20	0.41	0.77	−0.20	0.27
Tl (1e)	−0.50	0.90	0.47	0.11	0.36	0.58	−0.11	0.19
(CO) ₄ RuEH (ax)								
B (2a)	−0.45	0.51	0.36	0.56	0.77	0.92	−0.56	0.61
Al (2b)	−0.49	1.10	0.68	0.29	0.41	0.97	−0.29	0.29
Ga (2c)	−0.49	1.01	0.63	0.28	0.42	0.91	−0.28	0.30
In (2d)	−0.45	1.07	0.68	0.23	0.37	0.91	−0.23	0.26
Tl (2e)	−0.40	0.99	0.60	0.16	0.32	0.76	−0.16	0.21
(Por)RuEH								
B (3a)	0.28	0.60	0.48	0.61	0.75	1.09	−0.61	0.56
Al (3b)	0.13	1.23	0.81	0.25	0.40	1.06	−0.25	0.24
Ga (3c)	−0.10	1.23	0.85	0.21	0.39	1.06	−0.21	0.20
In (3d)	0.18	1.22	0.82	0.19	0.35	1.00	−0.19	0.19
Tl (3e)	0.30	1.14	0.74	0.10	0.29	0.84	−0.10	0.12

^a Partial charge q . ^b Sum of the orbital populations of the p_x and p_y orbitals of E in the complexes. ^c Orbital populations of the p_z orbitals of E in the complexes. ^d Electron transfer from the ligand EH to Ru regarding the σ -contribution: difference between $q(\text{EH})$ and $\Delta q(\pi)$. ^e Electron transfer from EH to Ru regarding the π -contribution: orbital population of the np_x and np_y orbitals of E in the complex. ^f Ratio of π -back-bonding (from Ru to EH) to σ -donation (from EH to Ru), given by $|\Delta q(\pi)|/|\Delta q(\sigma)|$.

was calculated at the central nickel atom in Ni(BMe)₄.¹² In contrast, for (Por)RuGaH (**3c**) we find a negatively charged ruthenium atom (−0.1 e). It is often stated (but sometimes debated) that the electronegativities of group 13 atoms follow not a smooth decreasing trend down the periodic table but often a zigzag behavior similar to the ionization potentials, which rationalizes such irregularities.³²

The atomic charges on E in (Por)Ru–EH and in both (CO)₄Ru–EH isomers show the same trend when going down the group 13 elements from boron to thallium. The atomic charge observed at the boron atom is always the least positive, while the others (Al–Tl) differ from each by only 0.1 e . Although atomic partial charges can sometimes be misleading with regard to the ionic contribution in the Ru–E bond, because the overall charge of an atom is not directed,¹² we suggest that the different charges can be explained qualitatively by the bonding models as shown in Figure 1.

Because the σ -donation of EH to the transition metal clearly outweighs the π -back-bonding contribution in the opposite direction, the formally neutral EH fragment will acquire a partial positive charge. Mixing in ionic contributions (Ru ^{δ^+} –E ^{δ^-}) will reduce the positive charge on E. The ionic contribution is expected to be most significant for the borylene compounds, and thus a lower positive charge is observed at BH relative to the heavier homologues. This qualitative explanation agrees with former calculations where the largest ionic contributions to the transition metal–group 13 bond were found for the borylene complexes.¹²

More quantitative statements can be drawn from looking at the NBO orbital population of the group 13 element E. The orbital population (Table 2) of the p_x and p_y orbitals ($p_{x,y}(\text{E})$) at the group 13 element E in L_nRu–EH (L_n = (CO)₄, Por), in which the Ru–E bond lies along the z -axis, reveals a significant population in contrast to the formerly empty p_π orbitals in the fragment EH. This difference is due to electrons transferred from the occupied ruthenium d_{xz} and d_{yz} orbitals into empty p_x and p_y orbitals at E (Figure 1), which will

be denoted as $\Delta q(\pi)$. A higher $\Delta q(\pi)$ value implies a stronger π -back-bond. $\Delta q(\sigma)$, calculated from the difference of $\Delta q(\pi)$ and the charge on EH in the complex $q(\text{EH})$, gives the σ -donation from the fragment EH to the ruthenium atom.

Independent of the ligands (Por, CO) and the geometry, $\Delta q(\sigma)$ and $\Delta q(\pi)$ both decrease from B down to Tl, as one expects from a decrease in the Ru–E bond dissociation energies due to a decreasing overlap between Ru and E with increasing nuclear charge of E. The only exception is a small increase of $\Delta q(\sigma)$ from B (0.92, **2a**) to Al (0.97, **2b**) in the axial carbonyl isomers. While all other values of $\Delta q(\sigma)$ decrease slightly from B to In, the Tl compounds show significantly lower values probably due to the relativistic 6s stabilization, which is partly responsible for the inert pair effect.³³ The $\Delta q(\pi)$ values decrease steadily from Al to Tl but show a markedly increased value for the boron analogues (about twice as big as for the Al complexes) due to a much higher π -back-bonding contribution. To make this more transparent, the ratio of π -bond back-donation to σ -bond donation at E ($b/d = |\Delta q(\pi)|/|\Delta q(\sigma)|$) is given in Table 2. Following the trend of $\Delta q(\pi)$, the b/d ratio decreases slowly from Al to Tl, and the boron analogues show again a significantly higher value due to the importance of π -back-bonding contributions. A similar result was reported by Frenking et al. for the iron tetracarbonyl complexes.²

For each group 13 element E, $\Delta q(\sigma)$ is the highest for (Por)Ru–EH (**3a–e**) and lowest for the equatorial carbonyl compounds (**1a–e**), while $\Delta q(\pi)$ remains basically the same. Therefore the highest b/d ratios were found for the equatorial carbonyl isomers (**1a–e**) followed by the axial isomers (**2a–e**). The porphyrin complexes (**3a–e**) show smaller values corresponding to a smaller percentage of π -back-donations compared to the σ -donations from E to Ru. However, compared to both carbonyl isomers, the porphyrin compounds exhibit similar absolute π -back-donation and stronger σ -donation bonds. In agreement with the enormously high bond

(32) Sanderson, R. T. *J. Am. Chem. Soc.* **1952**, *74*, 4792.(33) See discussion in: Schwerdtfeger, P.; Heath, G. A.; Dolg, M.; Bennett, M. A. *J. Am. Chem. Soc.* **1992**, *114*, 7518.

dissociation energy of the porphyrin borylene (**3a**) the $\Delta q(\sigma)$ (1.09) and $\Delta q(\pi)$ (-0.61) values are the largest within the calculated complexes. Similar values were observed from former calculations of the iron carbonyl borylene $(\text{CO})_4\text{FeBH}$.¹⁰

Summary and Conclusions

Density functional calculations have been used to examine the ruthenium group 13 element bond in the porphyrin compounds $(\text{Por})\text{Ru}-\text{EH}$ (**3a-e**) and $(\text{Por})\text{Ru}-\text{E}(\text{trip})$ ($\text{E} = \text{B-Tl}$, **4a-e**). For comparison reasons, the equatorial (**1a-e**) and axial carbonyl compounds $(\text{CO})_4\text{Ru}-\text{EH}$ (**2a-e**) have been calculated as well. The calculations predict very short Ru-E bond lengths for the porphyrin compounds, more than 10 pm shorter than the corresponding carbonyl complexes. This can be interpreted in terms of a higher degree of ionic character in increased bond strength present in $(\text{Por})\text{Ru}-\text{ER}$ ($\text{R} = \text{H}$, trip). Similar results have been reported for homolytic $\text{Fe}(\text{EMe})_5$.¹² Regarding the group 13 element E, the bond length increases down the row ($\text{B} < \text{Al} \approx \text{Ga} < \text{In} < \text{Tl}$) within all calculated compounds. The bond dissociation energies decrease down the group ($\text{B} > \text{Al} > \text{Ga} > \text{In} > \text{Tl}$), and for a given

element E ranging from Al to Tl we find similar dissociation energies for the carbonyl isomers compared to the porphyrin compounds. In contrast, much higher bond dissociation energies are calculated for the borylene complexes, especially for both the porphyrin borylene species **3a** and **4a**. Our NBO analysis is in agreement with these predictions and shows that the σ -donations ($\text{Ru}-\text{E}$) and π -back-donations ($\text{Ru} \rightarrow \text{E}$) for $(\text{CO})_4\text{Ru}-\text{EH}$ (**1a-e**, **2a-e**) and $(\text{Por})\text{Ru}-\text{EH}$ ($\text{E} = \text{B-Tl}$, **3a-e**) decrease down the row ($\text{E} = \text{B-Tl}$), as do the bond dissociation energies. The borylene compounds (**1a-3a**) exhibit the most significant back-bonding contributions.

Overall, the results clearly show that ruthenium porphyrin diyl compounds, containing sufficient protection to shield the group 13 element, can be expected to be stable both kinetically and thermodynamically, especially in the case of the borylenes. This makes them an attractive synthetic target.

Acknowledgment. T.B. and H.L.H. are grateful to the Alexander von Humboldt-Foundation (Bonn) for a Feodor Lynen Fellowship.

OM020530Z